1996A&A...314..599K

Astron. Astrophys. 314, 599–608 (1996)

ASTRONOMY AND ASTROPHYSICS

Long-term spectroscopic monitoring of BA-type supergiants

II. High-velocity absorptions in β Ori and HD 96919*

A. Kaufer[1], O. Stahl[1], B. Wolf[1], Th. Gäng[1,3], C.A. Gummersbach[1], I. Jankovics[2], J. Kovács[2], H. Mandel[1], J. Peitz[1], Th. Rivinius[1], and Th. Szeifert[1]

[1] Landessternwarte Heidelberg-Königstuhl, D-69117 Heidelberg, Germany
[2] Gothard Astrophysical Observatory, H-9707 Szombathely, Hungary
[3] STScI, Homewood Campus, 3700 San Martin Drive, Baltimore MD 21218, USA

Received 19 December 1995 / Accepted 17 March 1996

Abstract. During our extended monitoring campaigns on late B and early A-type supergiants (Kaufer et al. 1996, Paper I) we have observed extraordinarily deep and highly blue-shifted absorption events in the Hα line. In this work, new time-series observations showing the most extreme cases of such events observed so far are presented for two objects, β Ori (B8 Ia) and HD 96919 (B9 Ia). The development of these high-velocity absorption (HVA) events in velocity and time are discussed: the HVAs show *no* signs of spherically symmetric mass-loss events with subsequent accelerated propagation into the wind. The absence of unshifted line emission in connection with the HVAs is especially indicative of the non-sphericity of the active circumstellar regions. Simultaneously with the blue-shifted absorption, red-shifted absorption is found in Balmer and metallic lines, primarily during the onset of the developing event, which clearly reveals the complex structure of the involved velocity fields. Mass outflow and mass infall are present in the envelope. As a picture for the circumstellar structures that cause the sudden appearance of the HVAs over a large velocity range, localized regions of enhanced mass loss on the stellar surface, which build up extended, rotating streak lines in the equatorial plane are suggested. Finally, the role of a critical ionization structure in the condensed structures is discussed.

Key words: stars: supergiants; mass loss; rotation; individual: β Ori; individual: HD 96919

1. Introduction

Our extended spectroscopic monitoring of late B and early A-type supergiants (Kaufer et al. 1996, Paper I; Stahl et al. 1995 describe the distribution of these data on CD-ROM) has shown for the first time the complexity of the Hα variability of these luminous objects. In Paper I mainly the general characteristics of the Hα variability were described with emphasis on the determination of typical amplitudes and time scales of variations at the base of the stellar wind, i.e. low velocities (typically up to ± 100 km s^{-1}). Hints for axisymmetric envelopes and rotational modulation of the lower wind regions rather than pulsation as source of the observed Hα variability were found. Further, in several cases suddenly appearing deep and highly blue-shifted absorptions in Hα were found and ascribed to a critical ionization structure of the wind.

In a new observing campaign over 120 nights in 1995, the most spectacular of these high-velocity absorption (in the following called HVA) events to date was observed in one of the stars of the sample of Paper I, namely HD 96919 (B9 Ia), cf. Fig. 4. Together with three similar but less strong events recorded in 1993 and 1994 in β Ori (B8 Ia) and in 1994 in HD 96919 we want to examine in this work the characteristics of such events and their physical implications for the structure of the extended envelopes of late B-type supergiants. In particular, we will consider whether the observed evolution of these absorptions is controlled by processes connected with the driving of the wind itself, or by rotation of two-dimensional structures across the observer's line of sight.

2. Observations

The observations of HD 96919 in 1995 were performed in the same way as described in Paper I for the years 1992–1994 at the ESO 50-cm telescope in La Silla, Chile with the Heidelberg echelle spectrograph FLASH. Between the 1994 and the 1995 run this spectrograph was upgraded to HEROS, the **H**eidelberg **E**xtended **R**ange **O**ptical **S**pectrograph, by adding a second, near-UV sensitive channel. The two channels are fed simultaneously by a dichroic filter located behind the echelle grating. Both channels are equipped with adapted cross dispersers and

Send offprint requests to:
A. Kaufer *e-mail*: A.Kaufer@lsw.uni-heidelberg.de

* Based on observations collected at the European Southern Observatory at La Silla, Chile

© European Southern Observatory • Provided by the NASA Astrophysics Data System

1996A&A...314..599K

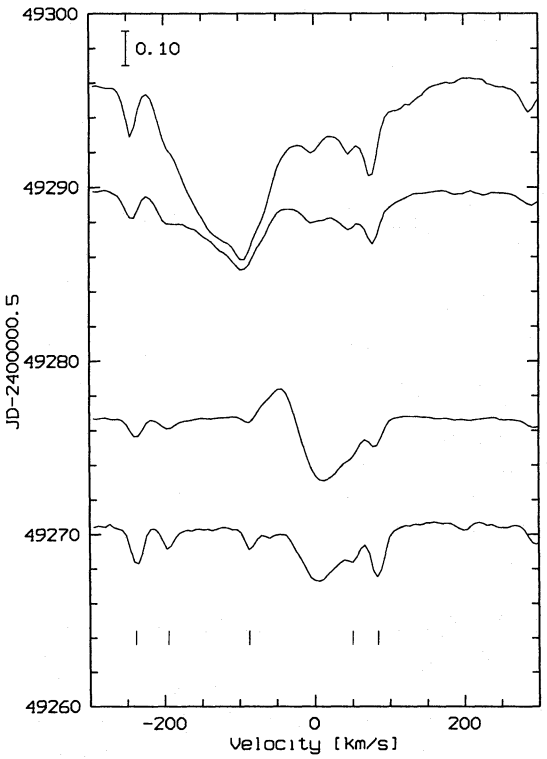

Fig. 1. Time series of spectra of Hα of β Ori obtained at the Landessternwarte in 1993. Due to the high water vapour content of the atmosphere above Heidelberg strong telluric lines are visible and have been marked.

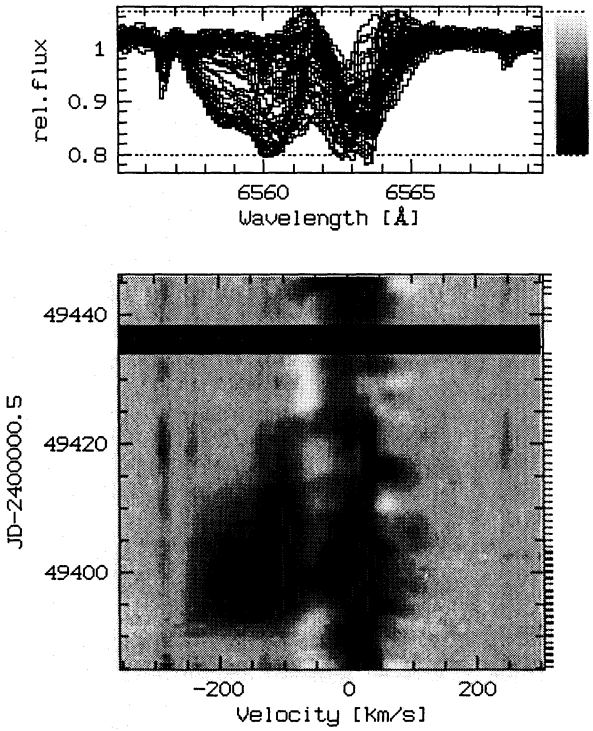

Fig. 2. Dynamical spectrum of Hα of β Ori in 1994.

CCD detectors covering 32 red and 63 blue orders resulting in a wavelength coverage of 3450 – 5560 Å and 5820 – 8620 Å, respectively, and a spectral resolution of $R \approx 20\,000$ over the whole wavelength range.

Table 1 shows the time spans of the observations and the number of spectra gathered over this time, together with the typical exposure time $t_{\rm exp}$ in minutes and the mean S/N in V of the time series. The time sampling was one spectrum per night for HD 96919; β Ori was observed in February to April twice per night with a separation of about 4 hours. The four spectra of β Ori in 1993 were taken with FLASH at one of the 70-cm telescopes of the Landessternwarte in Heidelberg and are nightly means from observations on October 9, 15, 28, and November 3, when 41, 9, 1, and 14 spectra were obtained, respectively. Luckily with these few snapshots the deepest HVA of β Ori was recorded but with poor time sampling.

The two channels of the HEROS spectrograph were reduced independently according to the echelle data-reduction procedures described in detail in Paper I.

3. High-velocity absorptions

Figs. 1 – 4 display the dynamical spectra or time series of spectra in the velocity interval of $\pm 300\,{\rm km\,s^{-1}}$ around the wind-sensitive Hα line of β Ori and HD 96919. All clearly display the high-velocity absorptions observed during the four observing campaigns. The dynamical spectrum of β Ori is composed of only the first 72 spectra we obtained, in order to focus on the time span of interest, i.e., the appearance and evolution of the event. The same holds for HD 96919 in 1994 where only spectra 58–68 are shown in Fig. 3. The velocity axis of all time-series plots are given for the rest wavelength of Hα. All dates in this paper are given as modified Julian date MJD = JD–2 400 000.5.

Table 1. Observing dates for the time series of spectra. The four spectra of β Ori in 1993 are nightly means from October 9, 15, 28, and November 3, where 41, 9, 1, and 14 spectra were obtained, respectively.

Object	Observation dates	Spectra	$t_{\rm exp}$ [min]	S/N
β Ori	Oct. 9 – Nov. 3 1993	4	5	300–1200
	Feb. 2 – May 31 1994	88	10	350
HD 96919	Feb. 3 – Jul. 1 1994	102	60	150
	Jan. 30 – Jun. 12 1995	91	60	220

In all four cases the HVAs are also found in the higher Balmer lines, but are strongly blended with their photospheric absorption profiles. Since comparatively undisturbed photospheric absorption profiles are available from the previous campaigns, we were able to subtract the photospheric part of the profiles, thereby leaving the HVA events more clearly visible. As template spectra we use the weighted averages of the time series of spectra showing no extraordinary events. The dynamical spectra of these difference spectra exhibit the HVA events

© European Southern Observatory • Provided by the NASA Astrophysics Data System

1996A&A...314..599K

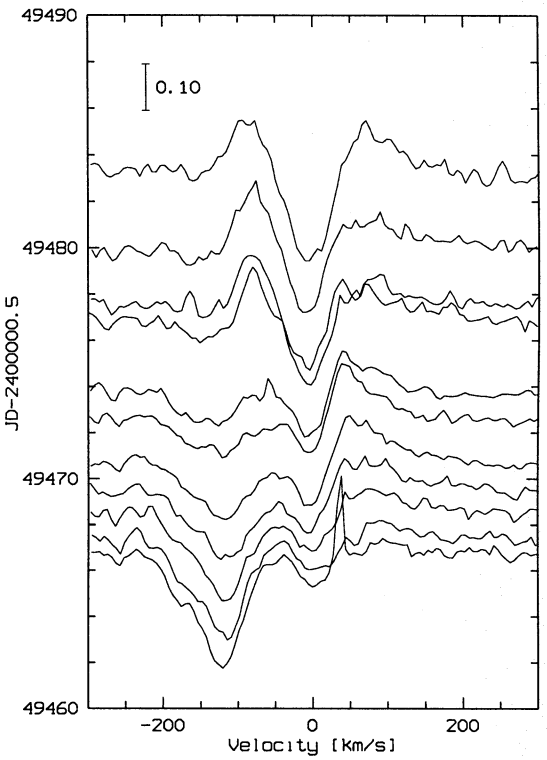

Fig. 3. Time series of spectra of Hα of HD 96919 in 1994.

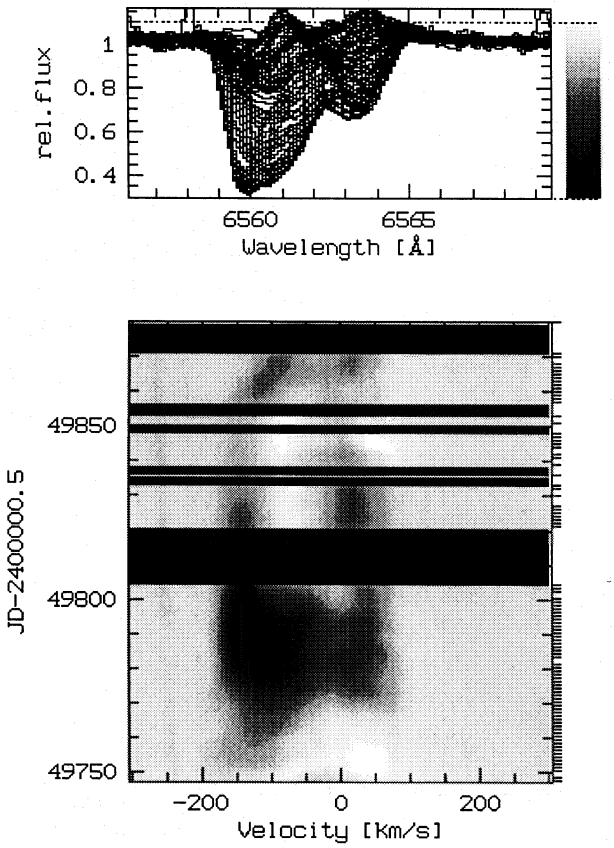

Fig. 4. Dynamical spectrum of Hα of HD 96919 in 1995.

Table 2. Characteristics of the HVA in Hα. All velocities are corrected for the systemic velocities, i.e. $v_{sys}(\beta\,\mathrm{Ori}) = +18\,\mathrm{km\,s^{-1}}$ and $v_{sys}(\mathrm{HD\,96919}) = -24\,\mathrm{km\,s^{-1}}$. For details on the different measurements see text.

	β Ori		HD 96919	
	1993	1994	1994	1995
MJD of max. blue depth	49295	49403	49466	49792
Max. depth in % of cont.	46	20	22	70
Vel. of max. depth [km s^{-1}]	−115	−139	−98	−108
Blue-edge velocity [km s^{-1}]	−238	−278	−210	−160
Red-edge velocity [km s^{-1}]	130	120	95	111
Max. W_λ[Å]	1.40	1.18	0.44	2.33
Undisturbed W_λ [Å]	0.07 ± 0.16		-0.42 ± 0.26	
Rise time of W_λ [d]	–	11	–	21
Decay time of W_λ [d]	–	20	–	46
Duration of event [d]	–	40	–	> 90

with the same pattern in velocities but with different absorption strength in the Balmer series (cf. Fig. 5), in the strongest wind sensitive FeII lines of multiplet 42 ($\lambda\lambda$5169, 5018), and (for the two strongest events in β Ori in 1993 and HD 96919 in 1995) also in the strong SiII$\lambda\lambda$6347, 6371 lines of multiplet 2.

3.1. Observational characteristics

In the following the characteristics of the observed absorption events will be described in detail with the aim of finding a common signature, which then should give hints to the physical mechanisms responsible for the appearance and time evolution of the HVAs. We first concentrate on the characteristics of the appearance of the absorption events and later discuss their time evolution.

Table 2 gives a compilation of the characteristic values measured for the four HVA events in the time series of Hα discussed in this section. Note that all velocities in this table are corrected for the systemic velocities taken from Paper I, Table 4.

As can be clearly seen from Fig. 1, 2 and 4 the HVAs develop simultaneously over a large velocity range from highly blue-shifted to considerably red-shifted, which indicates that a large portion of the absorbing volume of the envelope contributes. In β Ori in 1993 this broad blue-to-red absorption is seen in the spectrum taken at MJD 49295 (Fig. 1), and in 1994 between MJD 49395 and MJD 49407 (Fig. 2); for HD 96919 in 1995 between MJD 49970 and MJD 49800 (Fig. 4).

It is seen that the maximum depth during the absorption event is found at blue-shifted velocities but a deepening of the profile around systemic velocities up to the red wing of the profile is also present. The blue-edge velocities of these events are well defined and reach substantial fractions of the terminal wind velocities of these objects. In the case of β Ori the blue-edge velocity of 1994 has a value of $-278\,\mathrm{km\,s^{-1}}$, which even exceeds the lower limit for the terminal velocity given in Paper I (which

© European Southern Observatory • Provided by the NASA Astrophysics Data System

1996A&A...314..599K

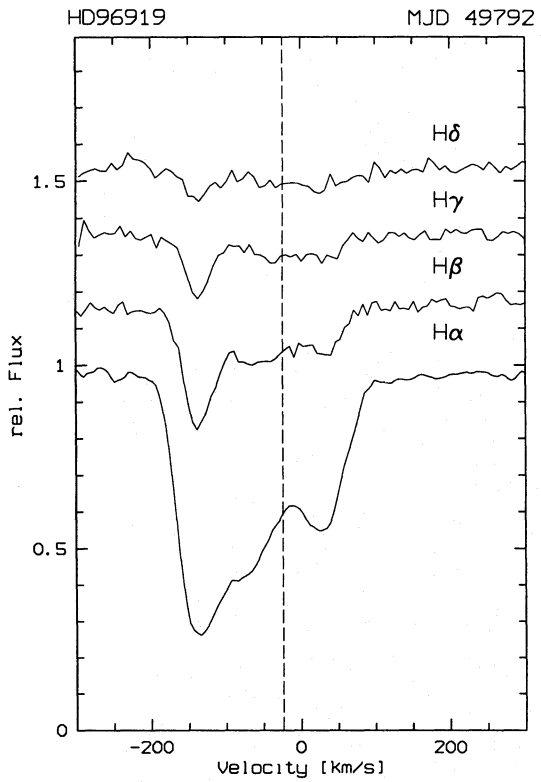

Fig. 5. Difference spectra of the Balmer series of HD 96919 at MJD 49792, i.e., when the blue absorption was deepest. The template subtracted from the spectrum was constructed from the time series from 1993, where no HVAs were observed. Note that the velocity of the maximum depth is constant for all Balmer lines but the absorption strength decreases for the higher Balmer lines.

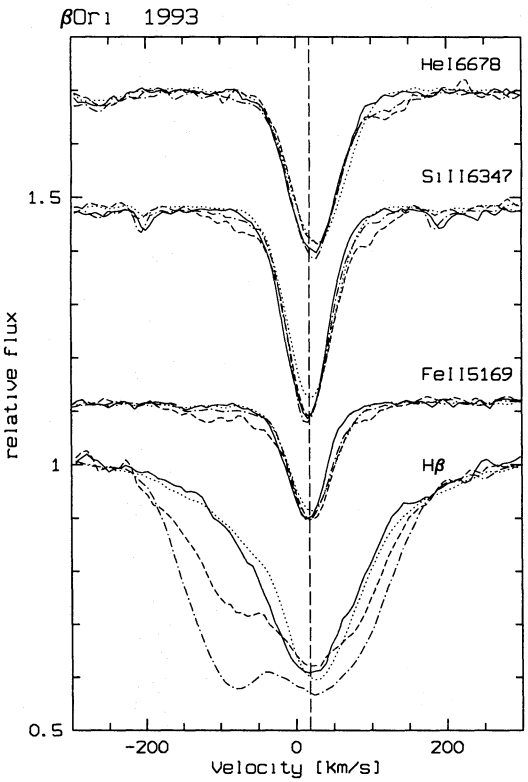

Fig. 6. Blue and red absorption in β Ori in 1993. Full line = MJD 49270, dotted = MJD 49276, dashed = MJD 49289, dot-dashed = MJD 49295. The vertical dashed line indicates the systemic velocity.

was derived from UV resonance lines showing admittedly quite ill-defined blue-edges).

The maximum depths of the blue HVAs are extremely large compared to any absorption observed during the extended monitoring programs reported in Paper I, indicating again that a large portion of the stellar disk must be covered by absorbing material of large column densities. In particular, the very deep and blue-shifted absorption in HD 96919 in 1995 (70% of the continuum absorbed at $-108\,\mathrm{km\,s^{-1}}$) raises the question whether such an event can be solely caused by a change of the ionization structure in the wind, as was suggested in Paper I for the fast developing events as in β Ori in 1994. Or is a locally enhanced mass-loss rate needed to increase the number of absorbers sufficiently to build up a circumstellar structure that produces such strong absorption events? This crucial point will be discussed below in Sect. 4.

The observed enhancement of the absorption from the systemic velocity to the red side of the profile extends surprisingly far into the wings of the Hα profiles. In the extreme case of β Ori in 1993 we find blue and red excess absorption clearly beyond $\pm v \sin i \approx 55\,\mathrm{km\,s^{-1}}$ even in 'bona fide' photospheric lines as shown in Fig. 6. In this figure the four observed spectra are displayed for the strongly affected Hβ line (the most sensitive line for circumstellar material in the optical range besides Hα) and for the FeIIλ5169, SiIIλ6347 and HeIλ6678 lines, which are expected to form a sequence in depth of line formation as well for the photospheric line core as for the wind-sensitive line wings.

In fact we see decreasing strength and extent of blue high-velocity absorption, along with increased and extended red absorption within this sequence. It is important to note that the maximum red and blue absorptions in the photospheric lines (dashed lines in Fig. 6) do not coincide with the maximum absorption in Hα, Hβ (dot-dashed line), and the higher Balmer lines, but that it is already observed in the spectrum taken 6 days earlier at MJD 49289.

Since only four spectra are available for this event we cannot follow the development of this extreme HVA in detail. Therefore, we inspected the well-sampled time series of HD 96919 in 1995 for a corresponding signature of blue and red absorption. In Fig. 7 four spectra of the same lines and with similar time sampling as in Fig. 6 are illustrated and in fact the same signature as described above for β Ori can be found. The red absorption is in this case less red-shifted and therefore is not discernible as a discrete absorption component, but as a strong broadening of the profiles to the red side.

Since a similar signature of blue–red absorption in the line profiles can be found, we follow the development with the help of the equivalent widths of the blue and

© European Southern Observatory • Provided by the NASA Astrophysics Data System

1996A&A...314..599K

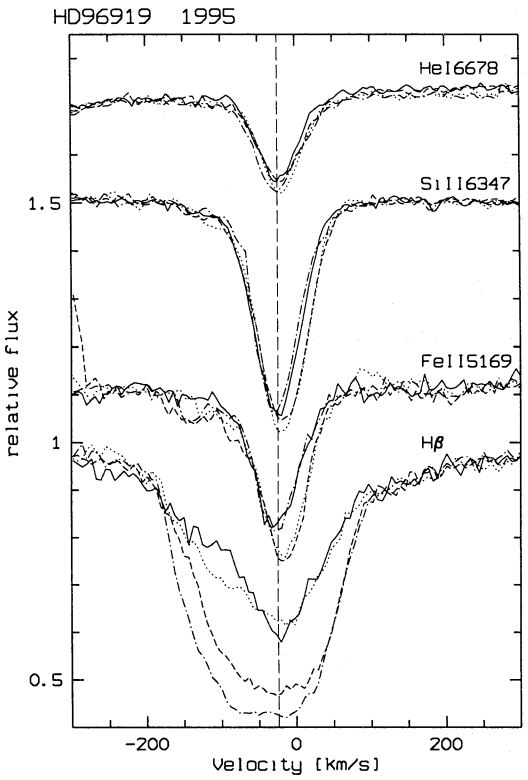

Fig. 7. Same as Fig. 6 but for HD 96919 in 1995. Full line = MJD 49748, dotted = MJD 49755, dashed = MJD 49769, dot-dashed = MJD 49775. Note that the time spans between the selected spectra were chosen similarly to those of the four spectra of β Ori in 1993.

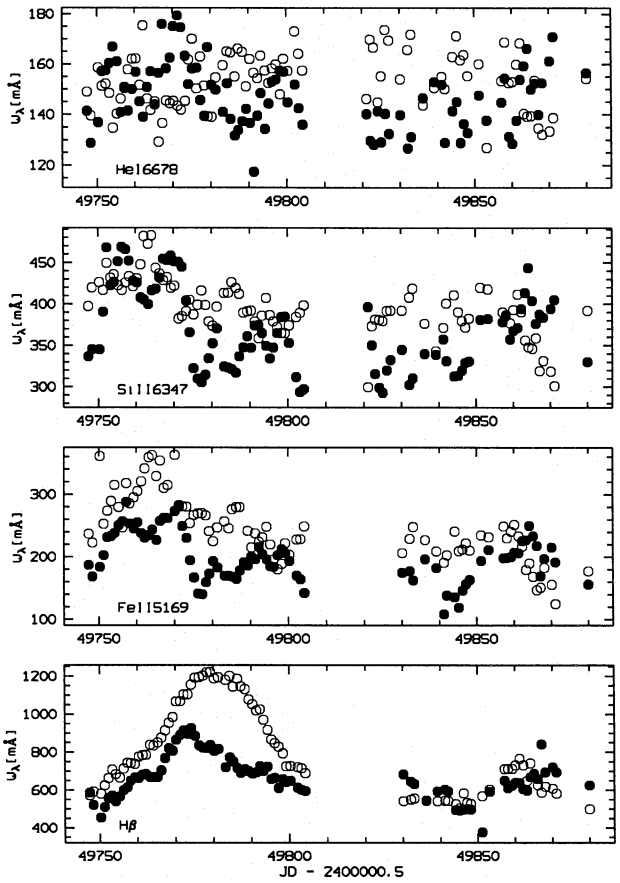

Fig. 8. Red (filled circles) and blue (open circles) equivalent-width curves of Hβ, FeIIλ5169, SiIIλ6347, and HeIλ6678 (bottom to top) for HD 96919 in 1995. Especially note the fast rise and decay of the red and blue absorptions during the onset of the HVA event (MJD 49770) in the metallic lines (admittedly barely visible in HeIλ6678) and the red wing of Hβ, together with the then still ongoing increase in the blue equivalent width of Hβ. Increased red equivalent width also becomes visible at MJD 49755 and MJD 49870 when the development of the blue absorption towards lower velocity is seen (cf. Fig. 10).

red sides of the different lines. Therefore, the equivalent widths of Hβ, FeIIλ5169, SiIIλ6347, and HeIλ6678 were integrated after making a linear continuum interpolation between a blue and red continuum window. These windows were chosen according to the spectral region around the lines where variability was observed, i.e. $-300, 300\,\mathrm{km\,s^{-1}}$ for Hβ, $-250, 180\,\mathrm{km\,s^{-1}}$ for FeIIλ5169, $-200, 200\,\mathrm{km\,s^{-1}}$ for SiIIλ6347, and $-180, 180\,\mathrm{km\,s^{-1}}$ for HeIλ6678. For the blue equivalent width the integration was performed between the blue window and the rest wavelength of the line corrected for the systemic velocity; the red equivalent width is the integral from this point to the red window. Fig. 8 shows the fast rise and decay of the red and blue absorptions during the onset of the HVA event (MJD 49770) in the metallic lines and the red wing of Hβ together with the then still ongoing increase in the blue equivalent width of Hβ. Increases in the red equivalent width also becomes visible at MJD 49755 and MJD 49870 when the development of the blue absorption is seen towards lower velocities (cf. below and Fig. 10).

As a third indication of the correlated occurrence of blue and red absorptions the Hα time-series of the B7 supergiant HD 91619 (Paper I, Fig. 3) has been inspected. In this case the depth of the red absorption even exceeds the depth of the HVA in the blue.

The simultaneous emergence of absorptions red-shifted and blue-shifted beyond $\pm v \sin i$, i.e., the rotational broadened profiles, requires the coexistence of approaching and receding absorbing material in front of the stellar disk, i.e., correlated mass infall and mass loss at least during HVA events.

Furthermore, blue-shifted emission peaks centered at $-60\,\mathrm{km\,s^{-1}}$ relative to the systemic velocity that preceded the HVA events are discernible in β Ori in 1993 around MJD 49276 and in 1994 at MJD 49393. In HD 96919 we find in 1995 at MJD 49754 a double-peaked emission symmetric about the systemic velocity at $\pm 60\,\mathrm{km\,s^{-1}}$. These emission peaks typically reach a 10% level above continuum. As shown in Paper I, variable double-peaked Hα emission that is symmetric about the systemic velocity is a common feature in late B and early A-type supergiants. The location of the variable emission was determined from the temporal variance spectra (TVS) and matches closely the positions of the emission peaks described above. The

© European Southern Observatory • Provided by the NASA Astrophysics Data System

1996A&A...314..599K

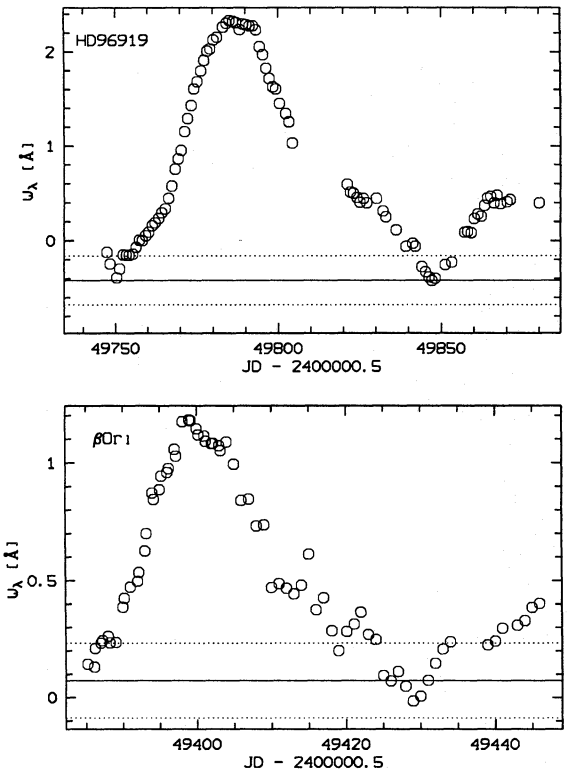

Fig. 9. Time development of the total Hα equivalent width during the HVA events of β Ori in 1994 (bottom) and HD 96919 in 1995 (top). For comparison the mean equivalent widths of the respectively preceding years are indicated by full lines. The broken lines indicate the corresponding standard deviations representing the usual Hα variability. These statistics were computed from 86 spectra of β Ori and 83 spectra of HD 96919 obtained in 1993 (cf.Paper I).

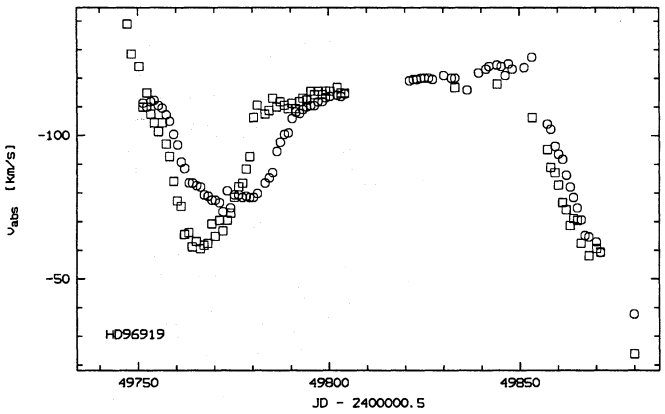

Fig. 10. Time development of the position of the deepest absorption in the HVA of HD 96919 in 1995. Circles are the measurements in Hα, squares in Hβ. Since in the latter case the absorption is strongly blended with the deep photospheric absorption profile, the HVA in Hβ was traced in the time series of difference spectra, which were created by subtracting the weighted-mean spectrum of 83 spectra from the year 1993 from each individual spectrum of 1995. In 1993 no HVAs were observed. Positions were measured by fitting Gaussians to the absorption components. Velocities are corrected for the systemic velocity.

observed variability was already ascribed to rotational modulation of surface structures. In the three cases discussed here, the observed emission peaks seem to be directly connected to subsequent HVA events.

3.2. *Time development*

The observed long-term development of the HVAs is of fundamental importance for the interpretation of these events. In Fig. 9 we first characterize this evolution by means of the temporal variation of the equivalent widths W_λ of the Hα profiles (integrated from 6554 to 6570 Å= $\pm$400 km s^{-1}). We restrict ourselves to the two well-sampled and well-covered events in β Ori in 1994 and HD 96919 in 1995. To demonstrate the strength of the HVA events, the mean equivalent widths of the time series when no HVAs were observed (i.e., for both objects in 1993 at La Silla) are indicated with full lines. The broken lines mark the corresponding standard deviations representing the 'normal' Hα variability. Note that the two panels cover different time spans and ranges in equivalent width – but also note the striking similarity in the run of W_λ, which might be a hint at a very general process that causes these extraordinary variations. The rise and decay times of the equivalent width, defined as the time spans from 10 to 90% of the maximum amplitude (counted from the undisturbed mean W_λ to the maximum W_λ) and back, are 21 and 46 days for HD 96919, and 11 and 20 days for β Ori, respectively. These rise and decay times manifest the strong ($\approx 1:2$) asymmetry of the time development, i.e., the fast appearance of the HVAs and the subsequent rapid deepening of the absorption over a large velocity range, followed by a long phase of fading of the absorption. The total duration of the two events is at least 90 days for HD 96919 and 40 days for β Ori, which corresponds to $0.75 \cdot P_{\rm rot}/\sin i$ and $0.38 \cdot P_{\rm rot}/\sin i$ if we use the the values for $P_{\rm rot}/\sin i$ derived in Paper I. These time scales for the development of the HVAs can be compared with the typical wind-travel time, which is of the order of 5 days if we compute the time to pass one stellar radius (115 $R_\odot$ for β Ori) with a typical expansion velocity of 200 km s^{-1}. This implies a length scale of a structure to develop or erode for β Ori in the order of only a few stellar radii.

The time development of the HVA in HD 96919 in 1995 needs some further discussion: in addition to the development discussed above we can see in Fig. 4 a narrow absorption enhancement migrating in the dynamical spectrum between MJD 49850 and MJD 49880 from -125 km s^{-1} to -35 km s^{-1}, i.e., towards the systemic velocity with increasing depth. This feature causes the final increase in the upper equivalent-width curve in Fig. 9 and in the red equivalent-width curves of Fig. 8. A trace of the positions of maximum absorption of this time series in Hα and Hβ is shown in Fig. 10. The steep decline in the velocity of this absorption feature at the end of the run is clearly seen. Interestingly, Fig. 10 also shows a very similar decline in the velocities at the beginning of the run, between MJD 49750 and MJD 49770. In both cases, the declines are preceded by

© European Southern Observatory • Provided by the NASA Astrophysics Data System

1996A&A...314..599K

double-peaked emission at $\pm 60\,\mathrm{km\,s^{-1}}$, i.e., close to $\pm v \sin i$, with a maximum emission at MJD 49754 and MJD 49847, respectively. It should be noted that these two double-peak emissions produce the two minima in the equivalent-width curve of HD 96919 (Fig. 9, top).

The reappearance of a pattern in the Hα variations has not been observed directly to date. But if we interpret this new observation in a quite natural way as the reappearance of an extreme circumstellar absorption structure after one corotation with the stellar surface, the rotation period would be defined by the time between the two emission events. This gives $P_{\rm rot} = 93$ days, which has to be compared to $P_{\rm rot}/\sin i = 119$ days from Paper I.

The maximum blue absorption in β Ori in 1993 was observed 108 days before the maximum of the HVA in β Ori in 1994. This interval is in exact agreement with the estimated $P_{\rm rot}/\sin i$ for this star. However, the (still unpublished) dynamical spectrum of β Ori of 130 days length obtained about three rotational cycles later does not show any remnants of the HVA activity.

4. Discussion: What do we see in the HVAs?

In this section, the sudden appearance and time development of the absorption enhancements will be discussed with respect to different circumstellar scenarios:

A mass-loss event at the base of the stellar wind with subsequent propagation into the wind.

Such a mass-loss event must be discussed from two points of view: on the one hand, it might be responsible for the sudden appearance of the HVAs due to radially outward directed propagation in the stellar wind on the typical flow-time scales. On the other hand, it might be the mechanism for the creation of a density enhancement in the wind that becomes visible at some rotational phases, as will be discussed below.

Rivinius et al. (1996) have recently used observations and detailed modelling to demonstrate that mass-loss variations at the base of the wind of early B hypergiants like ζ^1 Sco (B1.5 Ia$^+$) become visible as propagating absorption features in Hα. Since the objects discussed here have larger radii and lower terminal velocities, the ejected and propagating absorption enhancements should be seen even more clearly. The only case of a propagating feature that has been observed was for HD 92207 in 1994, where a slowly accelerating discrete absorption component could be followed over 150 days (cf. Paper I).

But this observation shows that the flow-time scales for the winds of BA supergiants are of the order of several weeks, which can also be seen by the integration of the beta-type velocity law appropriate to radiation-driven winds with typical stellar-wind parameters (with $\beta \approx 0.8 \ldots 1.5$ and $v_\infty \approx -200 \ldots -300\,\mathrm{km\,s^{-1}}$ the flow time scales defined as the time span for the acceleration from $0.2\,v_\infty$ to $0.8\,v_\infty$ are 20 to 60 days).

The HVAs obviously do not show the expected acceleration outwards in the wind. As already stated several times the HVAs appear simultaneously (at least much faster than the flow time scale) over a large velocity range – a characteristic not compatible with radial acceleration.

No broad emission excess symmetric about the systemic velocity accompanies the deepening of the blue-shifted absorption, as would be expected for a spherically symmetric mass-loss enhancement at the base of the wind, i.e., *no* P Cygni-type Hα profile becomes visible. Therefore, the possible mass-loss event would have to be concentrated to the equatorial region of the star – a situation which is also supported by the partially double-peaked emission features with a 10% intensity above the continuum, that are observed to precede the HVA. From the general characteristics of the Hα variability analyzed in Paper I, axial symmetry of the active and variable circumstellar structure of these stars was already derived. In an axisymmetric geometry of the envelope the unshifted emission component of a P-Cyg profile is strongly suppressed due to the lack of the emitting 'polar caps'.

The simultaneous presence of red-shifted absorption with the HVA events (cf. Fig. 6) suggests receding absorbing material in front of the stellar disk, which in fact must be due to infall of material onto the star. In particular, the observation of increasing red-shifted absorption beyond $+v \sin i$ in photospheric lines with increasing depth of formation supports the interpretation of the observed velocity field as mass infall. Again the non-existence, in this case of inverse P-Cyg profiles, can be attributed to the non-sphericity directed to the observer of the active region.

Effects in a critical ionization structure of the envelope, i.e., a switching from a fully ionized to a recombined wind structure.

This scenario has been suggested in Paper I mainly based on arguments considering the short time scale of the observed HVA events that had been observed then. The recombination-time scale of a typical late-B supergiant wind is of the order of 1 day in the Hα-forming part of the wind – a time scale not even properly resolved by our time series, which therefore means that an ionization structure would appear more or less instantaneously. Further, the ionization structure of the wind was estimated to be critical with respect to the ratio of ionizing photons to the number of recombinations in the wind. The primary uncertainty in the ionization structure comes from the uncertainties of the Lyman continuum, which is also strongly affected by mass-loss effects as shown by Najarro et al. (1996).

Since the HVAs are observed simultaneously in optical lines of HI, FeII, and SiII with comparable ionization potentials of 13.54, 16.16, and 16.27 eV, respectively, the ionization structures of these ions have to be considered: the majority of the metallic species should be doubly ionized in the wind in order to recombine and produce enhanced absorption in the singly ionized ions.

According to Abbott (1982) this transition between ionization stages, and therefore the transition between dominant driving lines is located in the effective-temperature region of late B supergiants. Such a decrease in the ionization stage might be due to an increased density in those regions (which increases the

© European Southern Observatory • Provided by the NASA Astrophysics Data System

1996A&A...314..599K

recombination rate), or to a lower temperature if the ionization balance is dominated by collisional ionization.

In addition Lamers et al. (1995) propose as an extension to this scenario the existence of a bistability mechanism mainly working at spectral type B1 and possibly also around B9: the recombinations result in less effective acceleration by lines, which in turn reduces the terminal velocity and increases the density of the wind. These changes cause even more recombinations, and give rise to absorption that might be observable as the sudden deepening of the HVAs. If this bistability mechanism applies, after the first recombination phase, the envelope structure will adapt to the new terminal velocity (i.e. the density structure) on the flow-time scale. This is compatible with our observations where the sudden onset over a large velocity range is followed by a gradual deepening of the blue absorption components.

The observed long-term development of the HVAs in this scenario can be due either to rotation of the azimuthally extended recombined structure in the envelope through the line of sight (see below), or to an intrinsic time development, i.e., the re-ionization and therefore dissolution of the absorbing region with time.

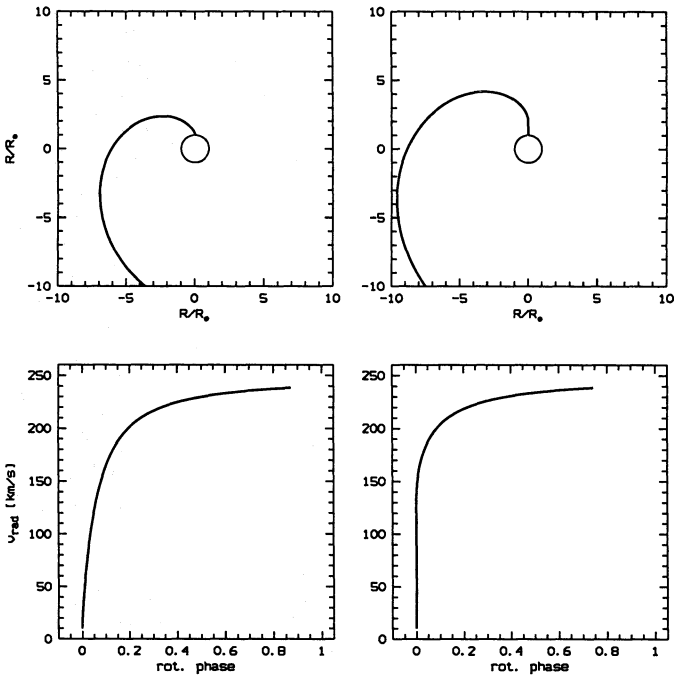

Fig. 11. Top: a streak line in the equatorial plane from material emitted from the stellar surface and accelerated according to a radial beta-type velocity law with $v_{\rm rad}(R) = 250\,{\rm km\,s^{-1}}(1 - R_\star/R)^1$. The azimuthal velocity accounts solely for the conservation of angular momentum with $v_\phi(R) = 60\,{\rm km\,s^{-1}} R_\star/R$ in the plot on the left. In the right panel, strict corotation up to 2 $R_\star$ was assumed. Bottom: The projected radial velocities on the central line of sight of the corresponding streak lines over the rotational phase. Phase zero is when the foot point of the streak line crosses the central line of sight. Note that strict corotation extends the velocity range coming almost simultaneously into the line of sight due to rotation of the streak line.

The rotation of already existing azimuthally extended density enhancements in the envelope into the line of sight.

From the time-series analysis of equivalent-width curves of Hα in Paper I, we have already concluded that rotational modulation and therefore weak magnetic fields may play an important role for the observed Hα variability at low velocities. The new detailed observation of the HVA event in HD 96919 in 1995 presented in this work, which possibly covers more than one rotational cycle and has an observable reappearance of the double-peak emission and decelerating blue absorption feature, fits quite well into the picture of rotating circumstellar matter. The same holds for β Ori, where two HVA events have been observed with a time interval of one rotational period.

In order to explain the fast rise of the HVAs over a large velocity range by the rotation of a circumstellar structure into the line of sight, this structure first has to rotate with the star with a radial rotational law that accounts at least for the conservation of the angular momentum. Furthermore, it has to be radially extended over the Hα-forming region in the envelope, i.e., several stellar radii. The motion of the absorbing material in this structure has to cover the observed, large range in radial velocity, even the positive velocities towards the star if we attribute the correlated red absorptions to the same structure.

Magnetic fields to enforce even a strict corotation of the structure up to several stellar radii would be of the order of a few Gauss if we adopt the model of Mihalas & Conti (1980) with typical stellar-wind parameters for late B supergiants. This model assumes corotation up to the Alfvénic radius. Therefore, the presence of weak magnetic fields would support the localization of the active region in the envelope.

A rough sketch of these two situations is given in Fig. 11. Assuming a rotating active region on the stellar surface, which emits material into the stellar wind, a streak line is formed due to the acceleration in the wind and the conservation of the angular momentum (cf. Mullan 1984 who discussed corotating interaction regions also for stellar winds in OBA supergiants, and Owocki et al. 1995 who use corotating wind streams to explain periodic variations in UV lines of the B0.5 Ib star HD 64760). The rotation of such an absorbing streak line into the line of sight would cause a sudden deepening over a large velocity range as can be seen from the development of the radial velocities of the streak line in the line of sight with the rotational phase (lower panel). With strict corotation close to the star due to weak magnetic fields the material would stay longer on a radial trajectory and the rise time due to the rotation into the line of sight becomes significantly shorter. Since the observed velocity field is complicated by the simultaneous presence of blue and red absorption components and the lack of observed acceleration, we cannot construct the shape of a real streak line emerging from an active stellar region.

In this scenario the observed long-term development of the HVAs is governed by the azimuthally extended density contrast, which follows a complex velocity field but is brought into the line of sight by rotation. Superimposed on this is the intrinsic

© European Southern Observatory • Provided by the NASA Astrophysics Data System

1996A&A...314..599K

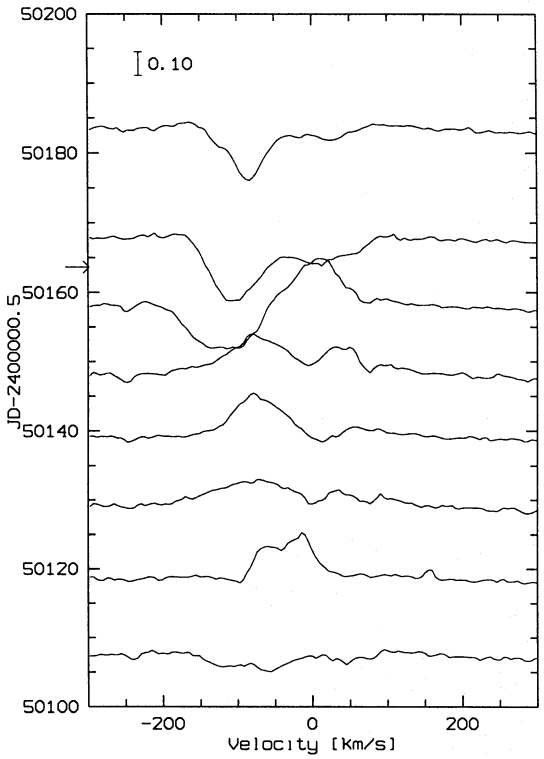

Fig. 12. Time series of spectra of Hα of HD 96919 from a HEROS campaign at La Silla in 1996.

time evolution of the structure. This intrinsic time development of the structure has to be considered since we have observed in the case of β Ori the strongest HVA in late 1993 followed by a weaker HVA one rotational cycle later in early 1994. But no remnant of this HVA was found about three rotational cycles later in the spectroscopic time series of 1995, which also covers at least one rotational cycle. Therefore, these structures must dissolve within few stellar rotations.

This scenario cannot constrain the mechanism creating the density enhancement in the stellar envelope. A localized mass-loss event and/or a change in the ionization structure as discussed above is still plausible.

5. Conclusions

Based on the high-resolution, spectroscopic time-series observations of several HVA events of various strength and duration in the late B-type supergiants β Ori and HD 96919, the development and origin of these mysterious features have been examined with the following main results:

- The observed HVA events are characterized by a similar morphology in the time development of the line profiles, which hints at a very general process that causes these extraordinary variations.
- The development of HVAs shows *no* signs of spherically symmetric mass-loss events with subsequent accelerated propagation into the wind. Non-sphericity in terms of active stellar regions determines the circumstellar structures observed in the HVAs.
- Regions of enhanced density can cause a transition of ionization stages in the wind, which can also produce enhanced absorption. In terms of the bistability mechanism the coupling of the driving lines to the terminal velocity can account for a further enhanced density.
- Localized regions of enhanced mass loss on the stellar surface can account for circumstellar structures with higher densities, which produce stronger absorption if they are located in the line of sight. Such active stellar regions can build up extended streak lines, presumably in the equatorial plane. The rotation of the streak line into the line of sight can account for the sudden appearance of the HVAs over a large velocity range.
- From the observation of correlated blue and red-shifted absorption we cannot be sure anymore about the existence of a purely radially outward accelerating velocity field in the lower circumstellar part of the envelope, as would be expected for a purely radiation-driven wind in the spherically symmetric case. Mass outflow and mass infall are present simultaneously.

Since rotation plays an important role for Hα-line formation in BA supergiants (as has been emphasized again in this work), the models for Hα-line formation in expanding envelopes including rotation as recently described by Petrenz & Puls (1996) for O stars are of great interest for these objects, too. The effects discussed by these authors are mainly of geometrical nature, i.e., the distribution of velocities and densities in the envelope due to the influence of rotation. Therefore, their models should also be applicable to the objects discussed here. The models display double-peaked Hα profiles, which strongly resemble the general Hα profiles observed in BA supergiants (cf. Paper I or the Hα-line profile of the A0 hypergiant 117-A in M33 by McCarthy et al. 1996).

BA-type supergiants are the visually brightest objects in a galaxy, and consequently they are potentially attractive distance indicators. For example, Kudritzki (1995) has recently described a new spectroscopic method of determining distances by using these stars and the wind-momentum – luminosity relation. Since the Hα line is the main diagnostic used to derive the stellar-wind parameters in this method, the effects of the observed variability as presented in this work and Paper I have to be discussed in order to judge the precision of the wind-parameter determination.

Acknowledgements. We would like to thank the European Southern Observatory for the generous allocation of observing time and the staff at La Silla Observatory for their kind assistance during the observations. We are particularly grateful to Prof. Schmidt-Kaler for making available the Bochum 60-cm telescope for 22 nights in 1994, Dr. C. Möllenhoff for providing a CCD system for the blue channel of HEROS in 1995, and Dr. A.W. Fullerton for carefully reading the manuscript. This work was supported by the Deutsche Forschungsgemeinschaft (Wo 296/16-1,2).

© European Southern Observatory • Provided by the NASA Astrophysics Data System

1996A&A...314..599K

References

Abbott D.C., 1982, ApJ 259, 282
Kaufer A., Stahl O., Wolf B., Gäng Th., Gummersbach C.A., Kovács J., Mandel H., Szeifert Th., 1996, A&A 305, 887 (Paper I)
Kudritzki R.-P., 1995, Quantitative Spectroscopy of Luminous Blue Stars in Distant Galaxies, In: Walsh J.R., Danziger I.J. (eds.), ESO-Workshop: Science with the VLT, Springer, p. 246
Lamers H.J.G.L.M., Snow T.P., Lindholm, D.M., 1995, ApJ 455, 269
McCarthy J.K., Lennon D.J., Venn K.A., Kudritzki R.-P., Puls J., Najarro F., 1995, ApJL 455, L135
Mihalas D., Conti P.S., 1980, ApJ 235, 515
Mullan D.J., 1984, ApJ 283, 303
Najarro F., Kudritzki R.-P., Cassinelli J.P., Stahl O., Hillier D.J., 1996, A&A in press
Owocki S.P., Cranmer S.R., Fullerton A.W., 1995, ApJL 453, 370
Petrenz P., Puls J., 1996, submitted to A&A
Rivinius Th., Stahl O., Wolf B., Kaufer A., Gäng Th., Gummersbach C.A., Jankovics I., Kovács J., Mandel H., Peitz J., Szeifert Th., Lamers H.J.G.L.M., 1996, submitted to A&A
Stahl O., Kaufer A., Wolf B., Gäng Th., Gummersbach C.A., Kovács J., Mandel H., Rivinius Th., Szeifert Th., Zhao F., 1995, The Journal of Astronomical Data 1, 3

Note added in proof: From the HVA event in HD 96919 in 1995 we were able to derive directly a rotation period of 93 days from the reappearance of double-peaked emission components within one time series. With this period, the reappearance of this extremely strong HVA after four rotational cycles was predicted for March 22, 1996 (MJD 50164 = time of the maximum blue absorption). Fig. 12 shows an Hα time series of HEROS spectra obtained with the ESO 50-cm telescope at La Silla around this time. This series clearly shows the reappearance of the strong blue absorption in perfect coincidence with the expected date, which is marked in the figure with an arrow. In addition, the symmetric double-peaked emission is clearly visible shortly before the blue absorption appears. This was found to be characteristic for all HVA events and is confirmed in this case again. This recent observation is a further very strong hint for corotating circumstellar structures in the envelopes of BA-supergiants as discussed in this work.

This article was processed by the author using Springer-Verlag LaTeX A&A style file *L-AA* version 3.

© European Southern Observatory • Provided by the NASA Astrophysics Data System